AUTHOR(S): AMOS, S., PRABHU, R. and NJUGUNA, J.

TITLE: Theoretical design and analysis of a sensing system for high pressure and temperature measurement in subsea underwater applications.

YEAR: 2017

Publisher citation: AMOS, S., PRABHU, R. and NJUGUNA, J. 2017. Theoretical design and analysis of a sensing system for high pressure and temperature measurement in subsea underwater applications. In Proceedings of the 60th MTS/IEEE OCEANS conference (OCEANS'17): a vision for sustaining our marine futures, 19-22 June 2017, Aberdeen, UK. New York: IEEE [online], article ID 8085023. Available from: https://doi.org/10.1109/OCEANSE.2017.8085023

OpenAIR citation: AMOS, S., PRABHU, R. and NJUGUNA, J. 2017. Theoretical design and analysis of a sensing system for high pressure and temperature measurement in subsea underwater applications. In Proceedings of the 60th MTS/IEEE OCEANS conference (OCEANS'17): a vision for sustaining our marine futures, 19-22 June 2017, Aberdeen, UK. New York: IEEE, article ID 8085023. Held on OpenAIR [online]. Available from: https://openair.rgu.ac.uk

Theoretical design and analysis of a sensing system for high pressure and temperature measurement in subsea underwater applications

Solomon Amos, Radhakrishna Prabhu, James Njuguna
School of Engineering, Robert Gordon University
Aberdeen, UK
s.u.amos@rgu.ac.uk

***Abstract*— The theoretical design and analysis of a metal coated hybrid sensing system of Fibre Bragg Grating (FBG) and Extrinsic Fabry-Perot Interferometer (EFPI) cavity for high pressure high temperature (HPHT) measurement in subsea underwater applications is reported. The FBG and EFPI are used to measure temperature and pressure respectively. An opto-mechanical model that assesses the measurement of HPHT for subsea underwater applications with hybrid sensing system was developed. In this model, coating of the sensor with metallic materials is studied. The model combines both optical and structural analyses for developing an optimal sensor system design. The optical analysis is carried out to obtain the spectral response of the sensor while the structural analysis is used to obtain the change in optical properties of the sensor due to photo-elastic effect. Analytical results showed that the temperature sensitivity of the hybrid sensor with double layer metal coated FBG increased to $23.89\ pm/°C$ when compared with single metal coated FBG of $13.95\ pm/°C$ from previous study and the associated pressure range measured up to $5000\ Psi$. Furthermore, the proposed sensor design has shown good linearity. While the single coated FBG sensor shows little sensitivity, the sensitivity increases with thickness for double metal coating.**

Keywords—Fibre Bragg grating; Extrinsic Fabry-Perot Interferometer; sensitivity; high pressure high temperature;

I. INTRODUCTION

The increasing demand in hydrocarbon production has led to a constant drive for the advancement in sensing technology with its ever increasing resolution, accuracy and stability. This has led to the development of downhole temperature and pressure gauges and optical fibre technologies for accurate measurement. The electrical sensors have many limitations when used as remote sensors in subsea underwater environments. For instance, the sensor head requires electrical cables to be connected to the remote location which are usually very difficult to provide. Also, sensitive elements of electronic components are needed for data processing in this harsh environment which affects the reliability of the sensor. One major challenge of the electrical sensors is that they become extremely unreliable when used in harsh environments [1].

Optical sensors have been proven to be more reliable, efficient and sensitive than their electrical counterparts [2-4]. Making them to become more widely acceptable by engineers and particularly attractive in the oil industry for subsea underwater environments. Also, as optical sensors are generally constructed using coated glass and metal, they have recently become the suitable choice in the oil and gas industry for deployment in harsh environments [3]. However, the optical fibre sensor suffers significant pressure and temperature cross sensitivity issue when used in oil and gas measurements. The different types of optical sensors are – fiber Bragg grating (FBG) for different parameter measurements [5-8], extrinsic Fabry-Perot interferometer (EFPI) for both pressure and temperature measurements [9-12].

A hybrid FBG/EFPI sensor based on single metal layer coating has been reported [11-13]. However, the single coated sensors suffer significantly from low sensitivity when used in elevated HPHT environments in the oil and gas industry. The sensitivity requirement of FBG sensors in oil and gas applications is very important and is usually in high magnitude.

Several techniques of metallic coating on FBG have been studied [13-16]. Some metallic coatings applied to optical fibre using techniques such as electroless plating, physical vapour deposition (PVD), and thermal spraying are silver, aluminum, copper, nickel, gold, titanium and lead. The electroless plating is the most commonly used method of coating because of its simplicity and low cost. Li *et al* [17] used lead cladding to enhance temperature sensitivity of FBG sensor. He found out that metal with much larger thermal expansion coefficient produces better sensitivity performance (five times more) than the bare fibre.

Silicon piezo-resistive and capacitive based pressure sensors have been reported and developed [18-20]. However, silicon based pressure sensors have suffered serious mechanical performance degradations when used in harsh environment.

A work on the preliminary investigation of temperature and pressure measurement system for downhole monitoring of oil wells using FBG/EFPI sensing had previously been reported to

overcome the issue of temperature and pressure cross sensitivity [21]. A de-multiplexing mathematical model was also proposed for separating the FBG spectrum from the EFPI. The FBG/EFPI sensor is a diaphragm based sensor with the referenced FBG to eliminate the effect of temperature cross sensitivity. However, with many advantages of this sensor type, it suffers low sensitivity when used in elevated temperature environments.

To overcome these limitations, this work presents an analytical model of metal coated hybrid sensing system of Fibre Bragg Grating (FBG) and Extrinsic Fabry-Perot Interferometer (EFPI) cavity for HPHT measurement in downhole monitoring applications. These sensors are made using two dissimilar metal materials and the sensors are spectrally encoded. Theoretical analysis was carried out to obtain the spectral response of the hybrid sensor and the structural analysis is used to obtain the change in optical properties of the sensor due to photo-elastic effect. Copper and nickel were chosen as the coating materials for this paper. While copper was selected as the outer protective layer due to its large thermal expansion coefficient and good extension, nickel was chosen as the conductive layer for its high melting point, non-susceptible to corrosion and oxidation, good conductivity and also large thermal expansion coefficient [22]. Silicon carbide (SiC) is the choice material for the EFPI diaphragm owing to its chemical inactiveness and mechanical robustness when used in harsh environment. The operating temperature of EFPI based pressure sensor is limited by the choice of the diaphragm being used. Here we propose a hybrid FBG/EFPI sensor with the FBG coated with outer protective layer of copper and inner layer of nickel. The EFPI has a SiC diaphragm.

II. ANALYTICAL MODEL

The schematic of the wavelength encoded hybrid sensor is shown in Fig.1. The sensing head is made up of FBG and EFPI sensors connected in series for HPHT measurements. The FBG is sensitive to temperature as a result of the thermos-optic effect and thermal expansion of the fibre material while the EFPI is used to measure high pressure. A convoluted combined signal is derived from the configuration but first, each individual signal was analysed and modelled.

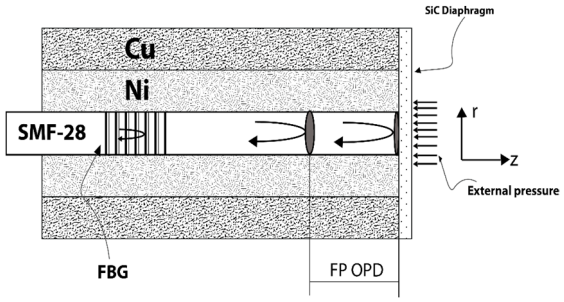

Fig. 1 Schematic representation of the proposed FBG/EFPI hybrid sensing head

To analyse the effect of the metal coating on the sensitivity of the hybrid sensor and obtain the optimum thickness of the coated metal, an opto-mechanical model will be developed. This model is based on the photo-elastic and thermo-optic properties of the fibres.

A. FBG sensor opto-mechanical model and response

The FBG sensor is wavelength encoded and the wavelength varies with the period of the grating. The FBG is produced by radiating the optical fibre with intense ultra-violet beams originated from the same laser source. The beams which are coherent, constructively and destructively interfere. The standard germanium doped FBG was used with wavelength of $1550nm$, the pressure sensitivity and temperature sensitivity are $-3pm/MPa$ and $13pm/℃$ [23, 24] respectively.
The opto-mechanical model of the FBG sensor predicts the shift in Bragg wavelength with respect to temperature and pressure functions at various thickness of the coated metals. To study the temperature sensitivity of a metal coated FBG, first the analysis of a coated FBG subject to the effect of strain by temperature changes is carried out.

The components of this system subject to both temperature and pressure are analysed numerically using Matlab. To measure temperature change ΔT, the wavelength shift $\Delta\lambda_B$ when exposed to thermal strain variation is given by [4]

$$\Delta\lambda_B = \lambda_B(\alpha + \xi)\Delta T + \lambda_B\left\{\varepsilon_z - \frac{n_{eff}^2}{2}[\nu(p_{11} + p_{12})\varepsilon_r + p_{12}\varepsilon_z]\right\} \quad (1)$$

where λ_B is the Bragg wavelength, n_{eff} is the effective refractive index of the fibre, p_{11} and p_{12} are the components of the fibre optic strain tensor also known as the Pockels constants of the fibre determined experimentally, ε_z is the applied strain along the longitudinal axis, ε_r represent the radial thermal strain, α is the thermal expansion coefficient for the fibre, ξ is the thermo-optic coefficient and ν is the Poisson's ratio.

To measure the combined effect of both temperature and pressure simultaneously, the shift in Bragg wavelength is expressed as [4]

$$\Delta\lambda_B = \Delta T.K_T + \Delta P.K_P + \Delta T\Delta P.K_{TP} \quad (2)$$

Where K_T, K_P and K_{TP} are the temperature sensitivity, pressure sensitivity and cross sensitivity respectively.

This model is based on some certain assumptions. The metal coatings, thermal expansion coefficient of the fibre α, the thermo-optic coefficient ξ and the Poisson's ratio ν are all constant and independent of the thermal variations. Also we assume that there is no relative displacement between the metal coating and the FBG.

To carry out the opto-mechanical model of the FBG sensor, the infinite circular thin wall of a hollow cylinder model is employed. This is made of three-layered materials with the first

material representing the copper coating, the second material representing nickel coating and the third representing FBG. The cylinder is considered to be an isotropic linear elastic composite material with free ends. The Lame's formula and strain-stress relationship is use in this model [25]. The parameters for the model are α_i for thermal expansion coefficient, E_i for Young's modulus, v_i for the Poisson ratio and r_i for radius of the fibre (i = 1, 2, 3 for the FBG, nickel and copper coating respectively).

Copper was used as the outer coat metal because of it physical property such as high thermal expansion, high ductility, good tensile strength, ability to withstand corrosion when use in harsh environment, strong resistance to creep (deformation) and has melting and boiling points of 1083.4 +/- 0.2°C and 2567°C respectively. The Young's modulus of Cu is between $110 - 128\ GPa$ and the Poisson ratio is 0.34.

The axial and radial characteristics of the metal coating are studied and analysed. From Hooke's theorem, the strain of the FBG as a result of the axial thermal stress is given by

$$\varepsilon_{1r} = v_1 K_1 \Delta T$$

Where K_1 is the thermal axial coefficient given by:

$$K_1 = \frac{(\alpha_3 - \alpha_1)E_3(r_3^2 - r_2^2) + (\alpha_2 - \alpha_1)E_2(r_2^2 - r_1^2)}{E_1 r_1^2 + E_2(r_2^2 - r_1^2) + E_3(r_3^2 - r_2^2)} \quad (3)$$

For FBG in the metal coated model, it is worth noting that the radial strain of the FBG as a result of the radial thermal stress, and the axial strain as a result of the axial thermal stress can are expressed as:

$$\varepsilon_{1r} = (1 - v_1)\frac{p_1}{E_1} \quad (4)$$
$$\varepsilon_{1z} = -2v_1\frac{p_1}{E_1}$$

The radial and axial strains can be expressed as:

$$\varepsilon_{1r} = \frac{1 - v_1}{E_1}K_2 \Delta T$$
$$\varepsilon_{1z} = \frac{-2v_1}{E_1}K_2 \Delta T$$

Where K_2 is known as the radial thermal stress coefficient expressed as:

$$K_2 = \frac{M_2 M_6 + M_3 M_5}{M_2 M_4 + M_1 M_5} \quad (5)$$

Where the respective expressions for M_i are shown in the table below

TABLE I. EXPRESSIONS FOR M_i

M_i	Expressions
M_1	$E_2(b^2 - a^2)(1 - v_1) - E_1 a^2(1 - v_2) - E_1 b^2(1 + v_1)$
M_2	$2E_1 b^2$
M_3	$E_1 E_2(b^2 - a^2)(\alpha_2 - \alpha_1)$
M_4	$2E_3(c^2 - b^2)a^2$
M_5	$E_2(b^2 - a^2)(1 - v_3)b^2 + E_2(b^2 + a^2)(1 + v_3)c^2 - E_3(c^2 - b^2)(1 + v_2)a^2 - E_3(c^2 - b^2)(1 - v_2)b^2$
M_6	$E_2 E_3(b^2 - a^2)(c^2 - b^2)(\alpha_2 - \alpha_3)$

The final strains ε_r and ε_z of the coated FBG are the combination of both the radial and the axial thermal stresses and it is expressed as:

$$\varepsilon_r = \left(\frac{1 - v_1}{E_1}K_2 - v_1 K_1\right)\Delta T$$

$$\varepsilon_z = \left(K_1 - \frac{2v_1}{E_1}K_2\right)\Delta T$$

Substituting these into the (1) the wavelength shift $\Delta\lambda_B$ when exposed to thermal strain variation;

$$\Delta\lambda_B = \lambda_B\left\{(\alpha + \xi) + (1 + p_{12})\left(K_1 - \frac{2v_1}{E_1}K_2\right) + \frac{n_{eff}^2}{2}(p_{11} + p_{12})\left(\frac{1 - v_1}{E_1}K_2 - v_1 K_1\right)\right\}\Delta T \quad (6)$$

$$\Delta\lambda_B = K_{mT}\lambda_B \Delta T \quad (7)$$

$$S_T = \alpha + \xi$$
$$S_z = (1 + p_{12})\left(K_1 - \frac{2v_1}{E_1}K_2\right)$$
$$S_r = -\frac{n_{eff}^2}{2}(p_{11} + p_{12})\left(\frac{1 - v_1}{E_1}K_2 - v_1 K_1\right)$$

Where K_{mT} is the sensitivity coefficient of the coated materials and optical fibre, S_T is the temperature sensitivity coefficient of the bare FBG whose constants are determined by the fibre material, S_z is the axial thermal strain sensitivity coefficient and S_r is the radial thermal strain sensitivity coefficients. The parameters M_1, M_2, M_3, M_4, and M_5 are affected by the properties of the FBG material.

B. The effect of metal coated FBG on temperature sensitivity

To properly investigate the effect of the metal coating properties on the sensitivity of FBG, the variation of temperature sensitivity and the material properties were first studied using the double layered opto-mechanical model shown in (7). In this design, a Cu-Ni coated FBG with diameter $62.5\ nm$ was used.

The parameters used for the simulation are listed as follow [26]; the FBG parameters are $E_1 = 74G\ Pa$, $\alpha_1 = 0.55 \times 10^{-6}$ /℃, $\xi = 6.3 \times 10^{-6}$ /℃, $p_{11} = 0.121$, $p_{12} = 0.27$, $n_{eff} = 1.456$, $v_1 = 0.17$, and $a = 62.5\ \mu m$.
The parameters for nickel coating are $E_2 = 220\ GPa$, $\alpha_2 = 14.2 \times 10^{-6}$ /℃, and $v_1 = 0.31$. The parameters for copper coating are $E_3 = 120\ GPa$, $\alpha_3 = 17.2 \times 10^{-6}$/℃, and $v_1 = 0.32$.

Fig. 2 presents the effect of the nickel metal coating property E_2 on temperature sensitivity of the metal coated FBG. As depicted in Fig. 2, the temperature sensitivity at first has a linear trend but has the tendency to decline with increase in elastic modulus. The temperature sensitivity varies from 20.57 pm/℃ to 21.79 pm/℃ at $E_2 = 180\ GPa$ and then starts to decline as E_2 increases further. This response is as a result of the linear structural properties of the metal coat and the linear characterization of FBG.

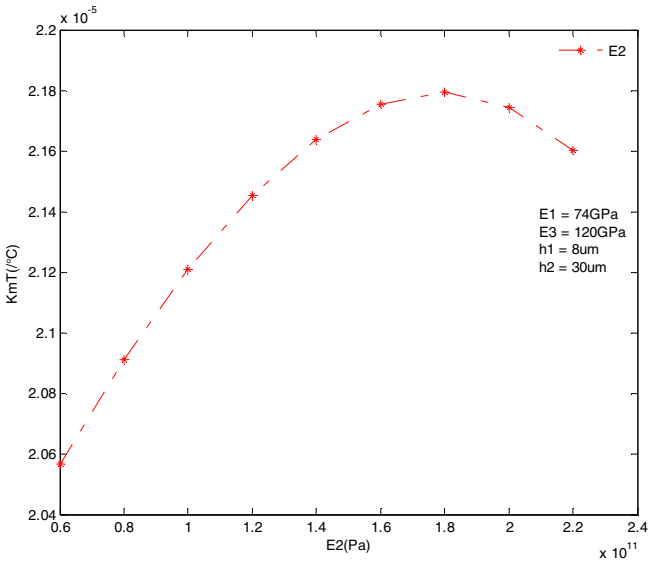

Fig 2. Effect of elastic modulus E_2 on temperature sensitivity K_{mT}

Also, Fig 3 depicts the effect of thermal expansion coefficient with temperature sensitivity. Within certain range, the temparature sensitivity increases with increase in coefficient of thermal expansion which shows a linear relationship. It is important to note that the material properties discussed above are interrelated. For example, the elastic modulus and the Poisson's ration are dependent on each other. If the elastic modulus increases, the Poisson's ratio decreases. Therefore, in a practical scenero, these properties cannot be separated from each other when studying the effects on the sensitivity of metallic coated FBG.

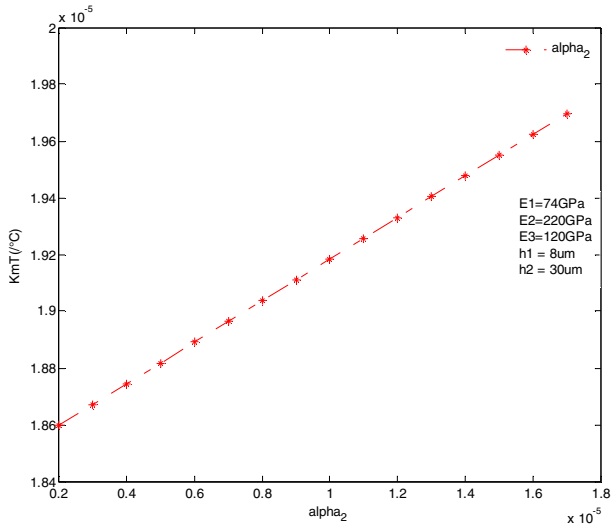

Fig. 3 Effect of thermal expansion coefficient α_2 on temperature sensitivity K_{mT}

The parameters for the $Cu - Ni$ coated FBG are shown above. The thickness of Ni is represented as $h2$ while that of Cu is $h1$. According to Fig 4, the $Cu - Ni$ coated FBG shows the relationship between temperature sensitivity with change in $h1$ and $h2$. It can be seen that when the coating thickness $h2$ is between 0 and 90 μm, the temperature sensitivity increases to $22.5 \times 10^{-6}\ /\ °C$ and then rises slowly to $23.6 \times 10^{-6}\ /\ °C$ before it reaches steady state at $23.89 \times 10^{-6}\ /\ °C$ with the increase of $h2$. This, compared with a single metal coated FBG having a temperature sensitivity of $13.9 \times 10^{-6}\ /\ °C$ as reported in [23, 24] , has higher temperature sensitivity for the same value of $h1$. The result shows that the double metal layer coated FBG enhances tempearture sensitivity more than a single layer coated FBG. The theoretical analyses show that the temparature sensitivity of FBG changes with the variation of metal coating thickness.

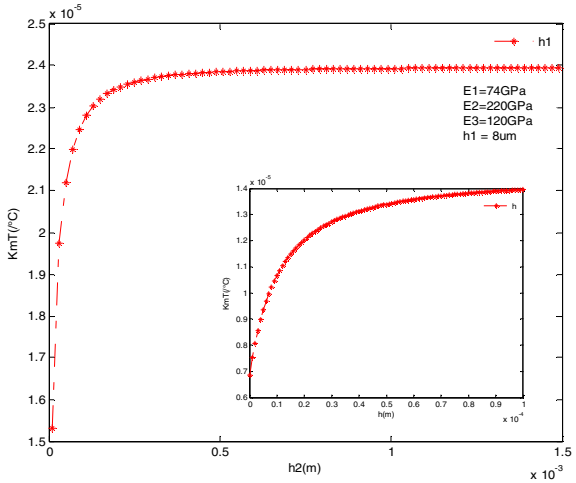

Fig. 4 Effect of metal coated FBG on temperature sensitivity. The inset showed the sensitivity on a single coated metal.

Fig. 5 shows the simulated response of a double metal coated FBG temperature sensitivity with single coated FBG. The temperature value used for the model ranges from $100 - 2000°C$.

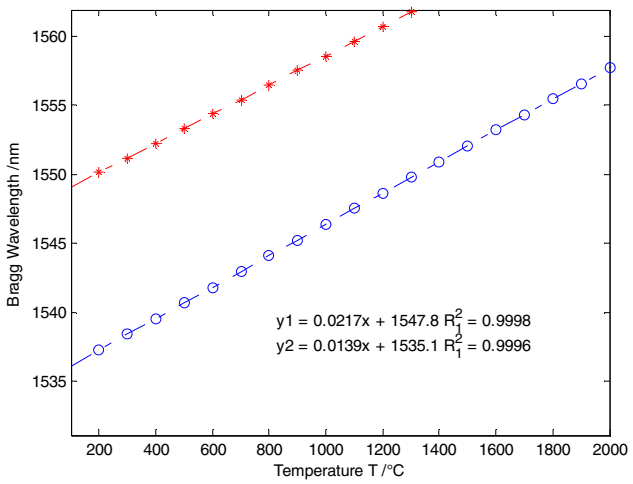

Fig. 5 Bragg wavelength shift as a function of temperature for double and single coated FBG

The simulation was done for different wavelength shifts and temperature variations to ensure repeatability and realiability. Results show that Bragg wavelength peaks increase linearly with various coating thickness. The double coated metal FBG peak wavelength increases linearly with a temperature sensitivity of $21.7 \times 10^{-6}/°C$ while that of single coated metal is $13.9 \times 10^{-6}/°C$. The result also showed that the Bragg wavelength shifted down by almost $12.7\,nm$. This shows that different variation of metal coated FBG thickness can be attributed to the change in temperature sensitivity and increase in the coated FBG thickness increases the the temperature sensitivity of FBG.

III. EFPI Sensor Model and Response

The EFPI is formed at the end face of the fibre and the SiC diaphragm. The SiC diaphragm deflects under any kind of stress which provides the pressure sensing characterization. The optical path distance known as the cavity length between the end face of the fibre and the diaphragm will change as a result of the lateral and longitudinal compressions of both the coating metals and the diaphragm. When the metal coated sensor head is subjected to an applied pressure, the longitudinal air-gap distance ΔL of the EFPI will change as a result. The relationship between the applied pressure ΔP and the cavity length ΔL of the hybrid sensor assuming the lead-in fibre and the reflecting diaphragm is expressed as [27];

$$\Delta L = \frac{3(1-\mu^2)r^4}{16Eh^3}\Delta P \qquad (8)$$

This models the deflection of a circular diaphragm when subjected to uniform distributed applied pressure.

Where r is the radius of the SiC diaphragm defined by the inner diameter of Cu coat metal, h is the thickness of the diaphragm, E is Young's Modulus and μ is Poisson's ratio of the diaphragm. The diaphragm pressure sensitivity (Y) is defined as the ratio of the deflection and pressure difference. The model is designed with $1\,mm$ diaphragm radius, $40\,\mu m$ thickness, $30\,\mu m$ cavity length and operates under pressure of upto $5000\,Psi$.

The relationship between the pressure sensitivity, the diaphragm thickness and its radius is depicted in Fig 6. It shows that pressure sensitivity increases with increase in diaphragm radius and decreasing thickness. Considering the design objective of the HPHT, the diaphragm radius is taken to be $1\,mm$ and the thickness to be $40\,\mu m$.

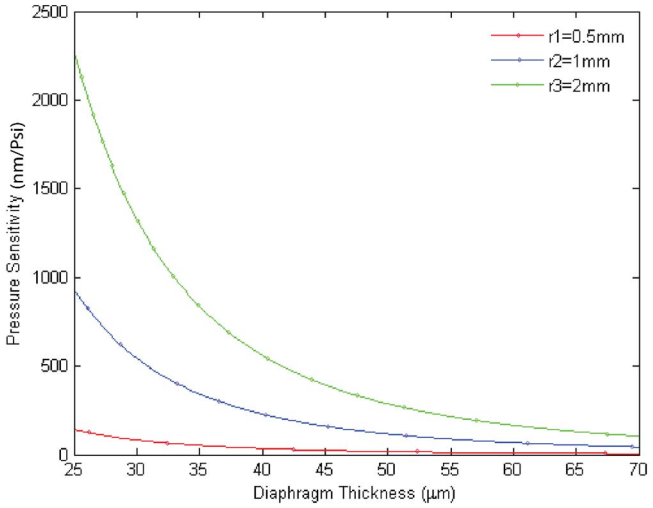

Fig. 6 Pressure sensitivity against SiC diaphragm thickness and radius. The sensitivity is directly proportional to the diaphragm thickness but inversely proportional to the square of the effective radius.

The frequency response of the SiC diaphragm against the thickness was also illustrated in this work. The frequency response is a very important performance parameter when dynamic pressure range is considered. For the SiC diaphragm to operate within a linear range of dynamic pressure, the resonance frequency should be at least three to five times the highest applied frequency [27].

Fig. 7 shows that the result of the EFPI pressure sensor model is feasible. The relationship between the cavity length and the applied pressure on the metal coated sensing head remains linear from theoretical modelling and predictions. It shows that the cavity length decreases linearly with increase in pressure from $0 - 5000\,Psi$. The cavity length of the proposed sensor can be affected by the physical properties of the coated metals used like the thermal expansion coefficient and the thickness of the SiC diaphragm. The variation of the cavity length against the applied pressure was measure as $21\,mm/kPsi$. However,

temperature compensation may be necessary for higher accuracy measurements.

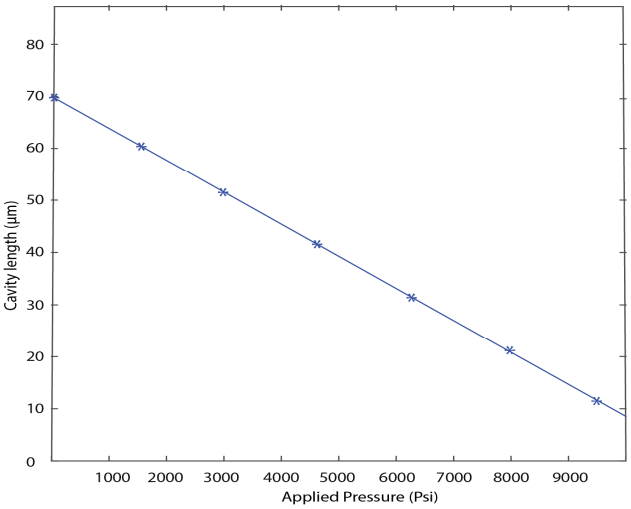

Fig. 7 Pressure sesponse as a function of cavity length.

The proposed sensor was highly dependent on the material properties of the diaphragm. SiC has a Young's modulus of 420GPa, making it very stiff and as such produced a very small deflection when the diaphragm was subjected to external applied pressure. It should also be noted that the sensitivity of the proposed sensor is dependent on the stability of the cavity length. Due to the nature of the SiC diaphragm, the cavity length tends not to drift over time which will enable the resolution and accuracy of the measurements to withstand long term reliability.

Furthermore, the requirement for any specific cavity length in EFPI sensor design, depends on the pressure range for the application. For subsea underwater applications, HPHT range measurements are required. Therefore, the proposed sensor design was carried out and could be used for reliable HPHT measurements in underwater applications. In this hybrid metal coated sensor design, there are few considerations to be noted. As a result of the usual high thermal expansion coefficient of metals, they may expand rapidly with higher temperature. Creeping tends to also occur on the metals with high temperature. These characteristics of the metals will have influence over the performance of the proposed sensor.

IV. CONCLUSION

This work detailed the description of a possible theoretical design of a hybrid FBG/EFPI sensor for measurements of temperature and pressure in subsea underwater applications. The FBG is coated with outer protective layer of copper and inner layer of nickel, while the EFPI pressure sensor has an all SiC diaphragm with $1\,mm$ radius, thickness of $40\,\mu m$ and cavity length of $30\,\mu m$.
Theoretical models and analysis of this sensor were carried out. The optical analysis is carried out to obtain the spectral response of the sensor while the structural analysis is used to obtain the change in optical properties of the sensor due to photo-elastic effect. Also, the characteristics of a rigidly SiC diaphragm is used to determine the suitability of the sensing configuration.

The sensor was theoretically designed for ranges of temperature and pressure between $100 - 2000\,°C$ and $0 - 5000\,Psi$ respectively. Simulations of these models were done and results show that temperature sensitivity of the sensor was enhanced from $13.95\,pm/°C$ to $23.89\,pm/°C$ and and the associated pressure range to be measured up to $5000\,Psi$ when compared to that of a single coated sensor.
The proposed hybrid sensor maybe useful for measurements of HPHT in subsea underwater applications.

ACKNOWLEDGMENT

The authors would like to thank Petroleum Technology Development Fund (PTDF) for sponsoring this research.

REFERENCES

[1] P. M. Nellen, P. Mauron, A. Frank, U. Sennhauser, K. Bohnert, P. Pequignot, P. Bodor, and H. Brändle, "Reliability of fiber Bragg grating based sensors for downhole applications," *Sensors and Actuators A: Physical,* vol. 103, pp. 364-376, 2003.

[2] K. T. V. Grattan and T. Sun, "Fiber optic sensor technology: an overview," *Sensors and Actuators A: Physical,* vol. 82, pp. 40-61, 2000.

[3] A. D. e. a. Kersey, "Optical Reservoir Instrumentation System," *Offshore Technology Conference,* vol. 2, pp. 469-472, May 1998.

[4] A. Othonos and K. Kalli, *Fiber Bragg gratings: fundamentals and applications in telecommunications and sensing*: Artech House, 1999.

[5] K. O. Hill, Y. Fujii, D. C. Johnson, and B. S. Kawasaki, "Photosensitivity in optical fiber waveguides: Application to reflection filter fabrication," *Applied Physics Letters,* vol. 32, pp. 647-649, 1978.

[6] B. S. Kawasaki, K. O. Hill, D. C. Johnson, and Y. Fujii, "Narrow-band Bragg reflectors in optical fibers," *Optics Letters,* vol. 3, pp. 66-68, 1978/08/01 1978.

[7] A. Kersey, M. A. Davis, H. J. Patrick, M. Leblanc, K. P. Koo, C. G. Askins, M. A. Putnam, and E. J. Friebele, "Fiber grating sensors," *Lightwave Technology, Journal of,* vol. 15, pp. 1442-1463, 1997.

[8] G. Meltz, W. W. Morey, and W. H. Glenn, "Formation of Bragg gratings in optical fibers by a transverse holographic method," *Optics Letters,* vol. 14, pp. 823-825, 1989/08/01 1989.

[9] W. J. Bock, W. Urbanczyk, J. Wojcik, and M. Beaulieu, "White-light interferometric fiber-optic pressure sensor," in *Instrumentation and Measurement Technology Conference, 1994. IMTC/94. Conference Proceedings. 10th Anniversary. Advanced Technologies in I & M., 1994 IEEE*, 1994, pp. 406-411 vol.1.

[10] J. Dakin and B. Culshaw, *Optical Fiber Sensors: Principles and components*: Artech House, 1988.

[11] J. A. Greene, T. A. Tran, K. A. Murphy, M. F. Gunther, R. G. May, and R. O. Claus, "Applications of the extrinsic Fabry-Perot interferometer," 1995, pp. 165-171.

[12] S. Webster, R. McBride, J. S. Barton, and J. D. C. Jones, "Air flow measurement by vortex shedding from multimode and monomode optical fibres," *Measurement Science and Technology,* vol. 3, p. 210, 1992.

[13] X. Li and F. Prinz, "Embedded Fiber Bragg Grating Sensors in Polymer Structures Fabricated by Layered Manufacturing," *Journal of Manufacturing Processes,* vol. 5, pp. 78-86, 2003/01/01 2003.

[14] L. Xiao Chun, P. Fritz, and S. John, "Thermal behavior of a metal embedded fiber Bragg grating sensor," *Smart Materials and Structures,* vol. 10, p. 575, 2001.

[15] S. Sandlin, T. Kinnunen, J. Rämö, and M. Sillanpää, "A simple method for metal re-coating of optical fibre Bragg gratings," *Surface and Coatings Technology,* vol. 201, pp. 3061-3065, 2006.

[16] Y. Li, Y. Wang, and C. Wen, "Temperature and strain sensing properties of the zinc coated FBG," *Optik - International Journal for Light and Electron Optics,* vol. 127, pp. 6463-6469, 2016.

[17] L. Gang-Chih, L. Wang, C. C. Yang, M. C. Shih, and T. J. Chuang, "Thermal performance of metal-clad fiber Bragg grating sensors," *IEEE Photonics Technology Letters,* vol. 10, pp. 406-408, 1998.

[18] H. Kapels, R. Aigner, and C. Kolle, "Monolithic Surface-Micromachined Sensor System for High Pressure Applications," in *Transducers '01 Eurosensors XV: The 11th International Conference on Solid-State Sensors and Actuators June 10 – 14, 2001 Munich, Germany*, E. Obermeier, Ed., ed Berlin, Heidelberg: Springer Berlin Heidelberg, 2001, pp. 56-59.

[19] W. H. Ko and Q. Wang, "Touch mode capacitive pressure sensors," *Sensors and Actuators A: Physical,* vol. 75, pp. 242-251, 1999.

[20] K. Petersen, P. Barth, J. Poydock, J. Brown, J. Mallon, and J. Bryzek, "Silicon fusion bonding for pressure sensors," in *IEEE Technical Digest on Solid-State Sensor and Actuator Workshop*, 1988, pp. 144-147.

[21] S. Udoh, J. Njuguna, R. Prabhu, B. Chirappuram, and P. Radhakrishnan, "Preliminary Investigation of Temperature and Pressure Measurement System for Down-hole Monitoring of Oil Wells Using FBG/EFPI Sensing Technique." *SPE Nigeria Annual International Conference and Exhibition August 4 - 6, 2015.*

[22] Y.-S. Choi, Y.-H. Yoo, J.-G. Kim, and S.-H. Kim, "A comparison of the corrosion resistance of Cu–Ni–stainless steel multilayers used for EMI shielding," *Surface and Coatings Technology,* vol. 201, pp. 3775-3782, 2006.

[23] R. Yun-Jiang, "In-fibre Bragg grating sensors," *Measurement Science and Technology,* vol. 8, p. 355, 1997.

[24] A. D. Kersey, M. A. Davis, H. J. Patrick, M. LeBlanc, K. P. Koo, C. G. Askins, M. A. Putnam, and E. J. Friebele, "Fiber grating sensors," *Journal of Lightwave Technology,* vol. 15, pp. 1442-1463, 1997.

[25] J. V. Uspensky and M. A. Heaslet, *Elementary Number Theory*: McGraw-Hill Book Company, Incorporated, 1939.

[26] Y. Feng, H. Zhang, Y. L. Li, and C. F. Rao, "Temperature Sensing of Metal-Coated Fiber Bragg Grating," *IEEE/ASME Transactions on Mechatronics,* vol. 15, pp. 511-519, 2010.

[27] D. Giovanni, *Flat and Corrugated Diaphragm Design Handbook*: Taylor & Francis, 1982.